[29]F. Linder and H. Schmidt, Seventh International Conference on the Physics of Electronic and Atomic Collisions, Amsterdam, 1971 (unpublished).

[30]C. A. Long and G. Ewing, Chem. Phys. Letters 9, 225 (1971).

PHYSICAL REVIEW A VOLUME 6, NUMBER 2 AUGUST 1972

Vibrational Excitation in N_2 by Electron Impact in the 15-35-eV Region*

Z. Pavlovic,† M. J. W. Boness, A. Herzenberg, and G. J. Schulz
Department of Engineering and Applied Science, Mason Laboratory, Yale University, New Haven, Connecticut 06520
(Received 18 January 1972)

The vibrational cross section by electron impact on N_2 exhibits a broad maximum near 22 eV. This maximum can be observed in the first three vibrational states, at all angles of observation. The angular distribution of the electrons having excited nitrogen to the vibrational states $v=1$, 2, 3 is measured. The shape of the angular distribution changes as the incident energy is varied from 20 to 28 eV. We interpret our observations in terms of the possible existence of a number of overlapping compound states above 20 eV.

I. INTRODUCTION

Compound states in molecules can be studied by measuring the structure in a variety of cross sections. Thus one can study the elastic, the rotational, the vibrational, the electronic cross sections, or even optical excitation or dissociative attachment. In principle, each of these "channels of decay" can give information on the existence of compound states.[1–6]

When the lifetime of the compound state is relatively long (e.g., larger than 10^{-14} sec), relatively sharp structures appear in many of the channels of decay. In such a case there is sufficient time available during the existence of the compound state for the nuclei to perform one or more vibrations so that vibrational structure in the compound state is evident. Decay of the compound state can take place not only to the ground vibrational state but also to higher lying vibrational states. Decay of a given compound state into as many as 13 vibrational states has been observed in H_2.[7]

When the lifetime of the compound state is *short* (i.e., 10^{-15}–10^{-14} sec) then the structure in any decay channel is broad, i.e., it is smeared out by the uncertainty principle. Such broad structures are often difficult to observe in the elastic cross section because the broad structure is superimposed on a large, energy-dependent, elastic cross section which results from "direct" scattering.[8] This channel of decay is, therefore, not easy to interpret. On the other hand, the "direct" scattering component is generally absent in vibrational excitation in homonuclear diatomic molecules because momentum transfer is unfavorable. Thus vibrational excitation is often the only decay channel which gives clearly information on short-lived compound states.

An example of the foregoing considerations is provided by the hydrogen molecule. The $^2\Sigma_u^+$ state of H_2^- is the lowest compound state in the hydrogen molecule. Its peak lies around 2–3 eV, and the state is about 2 eV wide. Vibrational excitation shows a well-developed peak in the region 2–3 eV,[9] but the elastic cross section is without noticeable structure.

In the case of the nitrogen molecule, a low-lying shape resonance[9,10] at 2.3 eV is well known and has been studied in great detail, both in elastic scattering and in vibrational excitation. In fact the vibrational cross section in the region 1.7–4 eV is dominated by the decay of this compound state. Sharp structure in the vibrational cross section for $v=1$ and $v=2$ exists also at higher energies (11.48, 11.75, 12.02 eV).[11]

The present study shows that even above the ionization potential of N_2 one can find short-lived compound states which, as one would expect from the foregoing discussion, decay into vibrational modes of the N_2 molecule. We present in this paper the energy dependence of the differential vibrational cross section for $v=1,2$, and 3 and also the angular distribution of the scattered electrons. These results indicate the existence of several indistinguishable short-lived compound states in the vicinity of 22 eV in N_2. This effect of several compound states is a new feature in these types of measurements. Comparison with the data of Trajmar, Cartwright, and Williams[12] on vibrational excitation in O_2 at 10 and 15 eV show that this phenomenon, the details of which are not completely understood, may exist in other molecules as well.

II. APPARATUS

A rotatable cylindrical electrostatic selector is used to produce a monoenergetic beam of electrons of small angular divergence which is crossed with a highly collimated molecular beam. The angular dependence and energy distribution of the scattered electrons are studied using a second electrostatic analyzer.

The apparatus is fundamentally similar to instruments previously employed in this laboratory[9] but does possess several refinements. A schematic diagram of the instrument is shown in Fig. 1. Electrons emitted from the thoria-coated hairpin filament are accelerated to 20 eV by the anode potential. The three-element aperture lens consisting of electrodes 4, 5, 6, is designed according to the theory given by Read[13]; it images aperture 1 onto the input aperture 7 of the monochromator, and it decelerates the beam to 2 eV. Aperture 3 forms the angular stop for the injection optics and limits the semiangle of the beam entering the monochromator to 5°. Because the divergence of the beam is restricted, electrons do not strike the cylinders forming the monochromator. This obviates the need for grids generally employed in monochromators of this type,[14] and thus simplifies construction. The inner and outer radii are 1.9 and 3.2 cm, respectively. The monochromator is rotatable from −10° to 120°.

A 2-eV beam of about 1×10^{-8} A and full width at half-maximum (FWHM) of 0.030 eV emerges from the monochromator and is focussed at the desired energy onto the molecular beam by the three-element lens system 10, 11, and 12. The impact energy is controlled by varying the potential between the first and third elements (electrodes 10 and 12) while the potential on the center element 11 is programmed to maintain a fixed focus. The resolution of the beam is measured by examining the width of the distribution due to elastic scattering or by measuring the widths of narrow resonances in the elastic scattering cross section; the position of several of these resonances which are now well documented[15] serve to establish the energy scale by performing experiments in a mixture of the calibration gas and the gas under investigation.

The fringing fields at the input and output planes of the monochromator and analyzer, which possess identical dimensions, are compensated for by applying the Herzog correction.[16] Thus we use a sector angle of 112° (instead of 127°), and we place the input and output apertures 0.25 cm from the ends of the cylindrical electrodes.

The molecular beam is formed by allowing gas to effuse from a fine fused-glass capillary array with pore size 0.0025 cm, thickness 0.05 cm, transparency 50%, and total diameter 0.15 cm. The pressure behind the array is maintained at a sufficiently low value such that the gas flow through the array is effusive. The existence of single-collision conditions in the interaction region is con-

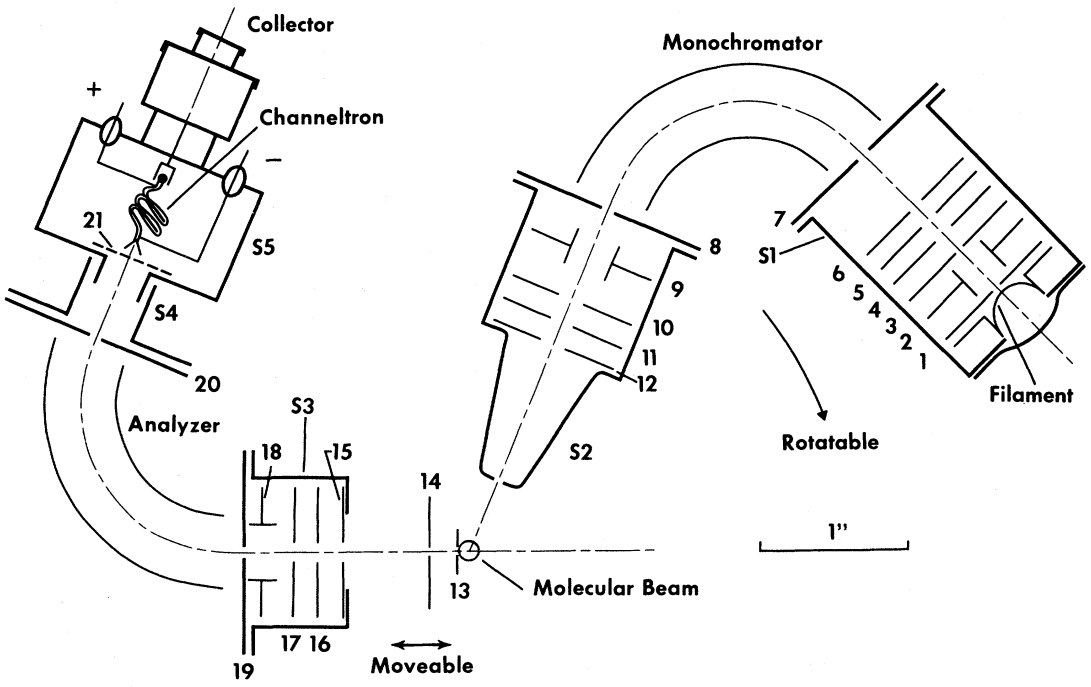

FIG. 1. Schematic diagram of double electrostatic analyzer.

firmed by demonstrating the linearity of the elastically scattered signal as a function of the background pressure in the vacuum system. This background pressure is monitored by a Bayard-Alpert ionization gauge mounted on the low-pressure side of the vacuum system. The array yields a pressure of 10^{-3} Torr in the collision region and is gold plated to avoid accumulation of scattered electrons.

Electrons scattered from the molecular beam enter the electron-optical system of the analyzer through the acceptance angle defined by apertures 13 and 14. Aperture 14 is moveable which permits the acceptance angle to be varied over the range from 2° to 6°. This feature is included to improve measurements of differential cross sections which vary rapidly with angle. Electrodes 15, 16, and 17 comprise a third three-element lens which focusses the electrons onto the input aperture of the analyzer and adjusts the energy of the beam to the desired analysis energy of 2 eV. Electrodes 2, 9, and 18 are perpendicular pairs of deflection plates whose potentials may be adjusted to compensate for mechanical misalignments and penetrations of stray fields. Shields $S1, S2, S3, S4$, and $S5$ restrict stray electrons and limit penetration of potentials from the various apertures into the collision region.

All parts of the instrument are constructed from molybdenum and cleaned by the etching process described by Rosebury[17]; adjacent parts are insulated by using 0.15-cm-diam sapphire spheres.

Magnetic fields are eliminated from the instrumental region by three pairs of mutually perpendicular Helmholtz coils approximately 30 in. in diam. The instrument is enclosed in a nonmagnetic stainless-steel vacuum chamber bakeable to 400 °C. A high-speed 6-in. oil diffusion pump, water baffle, and liquid-nitrogen trap enable an ultimate vacuum of 5×10^{-10} Torr to be achieved after baking the system for 24 h.

Electrons emerging from the exit aperture of the analzyer 20 are detected by a Bendix helical channeltron multiplier. A 90% transparent grid 21 prevents penetration into the electrostatic analysis region of the high voltage applied to the channeltron multiplier. Shields $S4$ and $S5$ eliminate signals from other directions from arriving at the multiplier. The background counting rate of the system is extremely low, only 5 counts per minute. Pulses from the collector are applied directly to the input of a charge-sensitive field-effect-transistor (FET) preamplifier which is maintained at a high voltage (2800 V). The output pulses are transformed to ground potential, amplified, shaped, amplitude limited by a single-channel analyzer, and the counting rate is measured with a scaler and ratemeter. For sufficiently high counting rates the analog output from the ratemeter is displayed on an X-Y plotter. Alternatively for low counting rates the pulses are taken to the digital input of a 1024-channel signal averager. The channel address of the signal averager is synchronized with the sweep voltage appropriate to the particular mode of operation of the instrument, so that successive sweeps are accumulated in the memory of the averager. This technique improves the signal-to-noise ratio in proportion to the square root of the number of sweeps. The counting rate of the system depends on the nature of the process being observed, and it varies between a few thousand counts per second to a few counts per minute. The latter requires signal accumulation using the averager for up to 24 h. After storage, the contents of the signal-averager memory are plotted on an X-Y plotter via a digital-to-analog converter.

III. RESULTS

The basic experiment that we perform using the double electrostatic analyzer measures the energy-loss spectrum, which exhibits well-pronounced peaks characteristic of the elastic and the first three vibrational cross sections. The simplest and most-reliable measurements consist of taking the ratio of the peak heights and studying these as a function of incident energy or angle of observation. Such a ratio eliminates all problems connected with focussing of lenses (whose focal length changes with energy) or imperfections of the apparatus as the angle is altered. We shall show below that considerable effort is necessary to obtain reliable *absolute* curves as a function of energy and angle of observation.

Energy Dependence of Ratio σ_v/σ_{el}

Figure 2 shows the ratio of the first vibrational peak ($v=1$) to the elastic peak, plotted in the energy range 2–35 eV, for three angles of observation. Two peaks are clearly evident; the first results from the well-known $^2\Pi_g$ shape resonance[9,10] in the neighborhood of 2.3 eV. The second peak is reported here for the first time. Since we are initially interested only in the broad features of this spectrum the data points are plotted at intervals of 2–3 eV; thus the resonant structure which we observe in the vicinity of 2 eV and also at 11.48 eV[18] is not included in Fig. 2. The peak is evident at all angles of observation. Since large vibrational cross sections often proceed via compound states in homonuclear diatomic molecules, we postulate that such may also be the case for the 22-eV peak.

It should be noted that Fig. 2 presents only the ratio of cross sections. In order to obtain the true, absolute, energy dependence of these cross sections, one has to make corrections for changes in the focal conditions of the electron optics as the

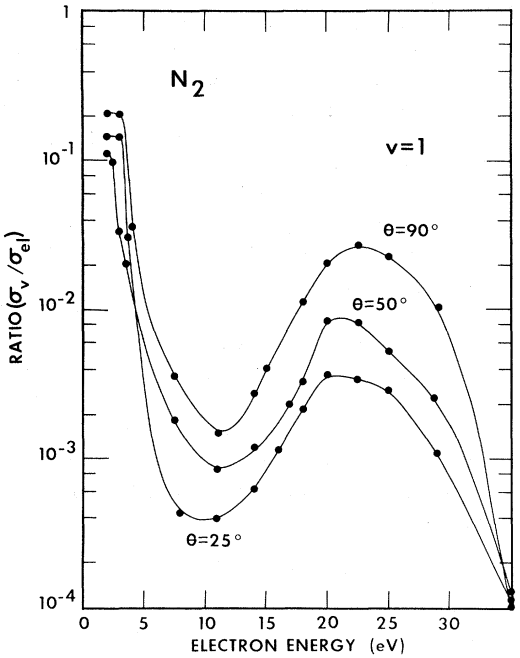

FIG. 2. Ratio of cross section to the first vibrational state of N_2 to elastic cross section (σ_v/σ_{el}) vs electron energy, for three angles of observation. The peak at 22 eV is interpreted in terms of broad overlapping compound states at that energy.

energy is swept. This can be accomplished in two ways: One can calculate theoretically the performance of the lenses and correct the measured points accordingly. Alternately, one may calibrate the apparatus on a cross section that is reliably known and correct the experimental readings accordingly. We found the latter approach more convenient and reliable, and we describe our procedure below.

Calibration Procedure

For calibrating our apparatus, we rely on the elastic cross section in helium as calculated by LaBahn and Callaway.[19] It is believed that this cross section is reliable to ± 5% but it is much better for angles larger than 30° for which the theoretical cross section agrees extemely well with experiment. Figure 3 shows the theoretical curve for helium, taken from the work of LaBahn and Callaway. All subsequent energy dependences reported in this paper are normalized to this curve.

For example, when we wish to measure the energy dependence of the elastic cross section in N_2 at a given angle (e.g., 30°), we proceed as follows: We measure the height of the elastic peak in N_2 at a given pressure. We then replace the nitrogen gas by helium and measure the elastic peak at the identical pressure.[20] We multiply the experimental ratio thus obtained $[\delta_{el}(N_2)/\sigma_{el}(He)]$ by the theoretical cross section to obtain the absolute value of the differential elastic cross section in N_2. The top curve of Fig. 3 shows the result of such a procedure, and it provides us with a "secondary standard" for the differential elastic cross section in N_2, traceable to the LaBahn and Callaway cross section in helium.

Comer and Read[11] measure the differential elastic cross section at an angle of 40° and 85° and obtain values of 6.3 and 1.8×10^{-16} cm^2/sr, respectively, around 11.5 eV. Their values are thus higher than ours by a factor of about 3. This discrepancy is not understood.

When we wish to measure the energy dependence of the vibrational cross section we proceed in a similar manner. We measure the ratio $\sigma_v(N_2)/\sigma_{el}(N_2)$ and multiply by the value of the "secondary standard", i.e., the value of the elastic cross section in N_2 shown in Fig. 3.

A small correction must also be made when measuring the angular dependence of any cross section. This effect is due to the fact that the collision volume, defined by the intersection of the molecular beam, incident electron beam, and the acceptance cone of the analyzer optics exhibits a small variation with the angle of observation. However, this correction is small and is at most

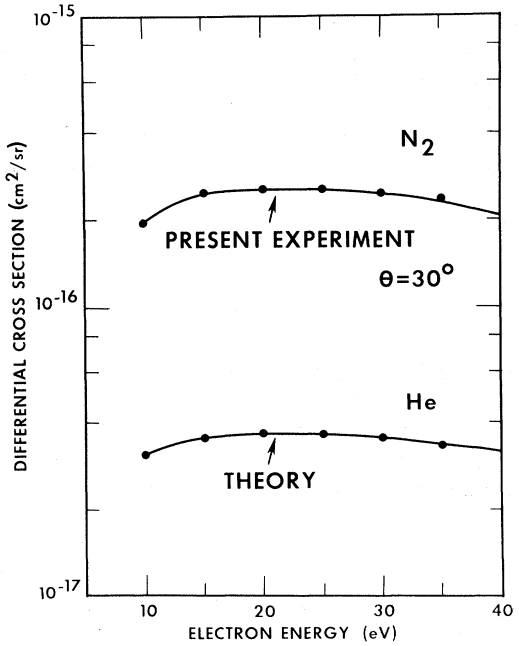

FIG. 3. Differential elastic cross sections at an angle of 30°. The bottom curve is taken from the theoretical work of LaBahn and Callaway and is used for normalization of the electron optics. The top curve is an experimental curve for N_2, normalized to the bottom curve. The top curve serves us as a secondary standard to which all other energy dependences are normalized.

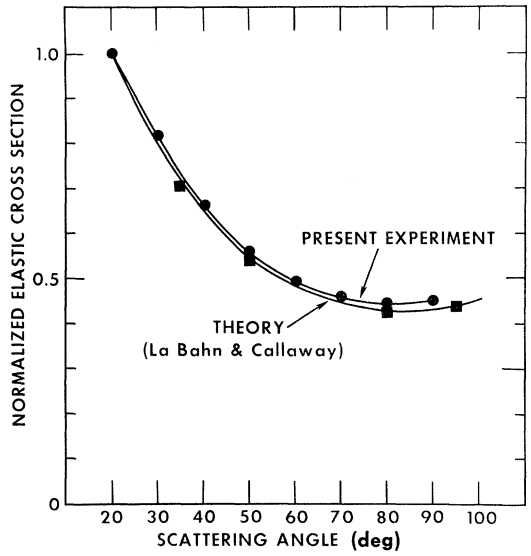

FIG. 4. Theoretical and experimental angular distributions at 25 eV in helium normalized at 20°. All subsequent angular distributions are corrected to the theoretical distribution of LaBahn and Callaway.

4%. Figure 4 shows the uncorrected, experimental, angular distribution in helium in comparison with the theory. All the angular distributions presented in this paper are normalized to the theoretical curve.

Energy Dependence of Absolute Vibrational Cross Sections

The energy dependences of the absolute vibrational cross sections for $v=1-3$ are shown in Figs. 5–7. All the vibrational cross sections show a relatively large peak near 22 eV, at all angles

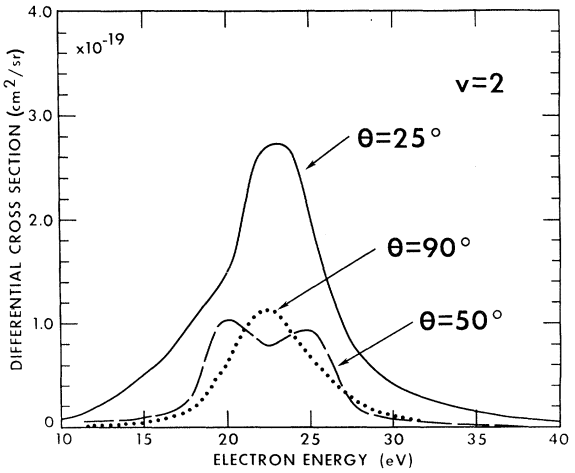

FIG. 6. Energy dependence of differential cross section for vibrational excitation to $v=2$, in N_2, for three angles of observation.

of observation. We cannot exclude the possibility that sharp structures are superimposed on the smooth curves shown. In fact, when we divide a 1-eV interval on the curve for $v=3$ between 20.7 and 21.7 eV into 1000 points and accumulate data for about 48 h, structure appears which is spaced about 200 meV apart. However, since the signal-to-noise ratio is only about 2–3, we cannot be completely certain about the existence of this structure, and thus we do not show it in Fig. 7.

Angular Dependence of Differential Cross Section

Angular dependences are shown in Figs. 8–11. Figure 8 shows the elastic cross section, in the range of energies 21.0–25.0 eV. Curves were taken at 0.5-eV intervals, but they are indistin-

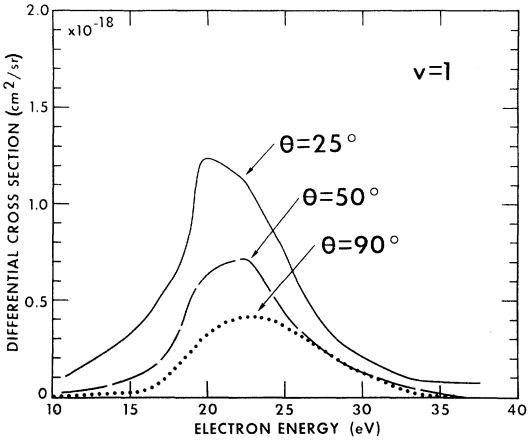

FIG. 5. Energy dependence of differential cross section for vibrational excitation to $v=1$, in N_2, for three angles of observation.

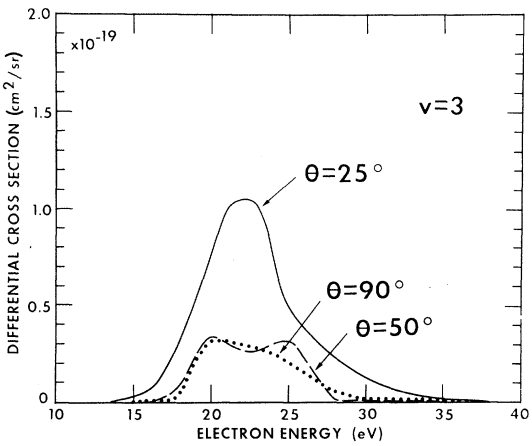

FIG. 7. Energy dependence of differential cross section for vibrational excitation to $v=3$, in N_2, for three angles of observation.

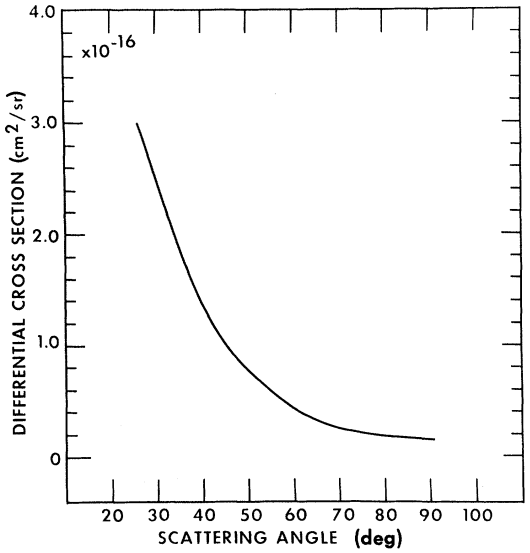

FIG. 8. Angular distribution of elastically scattered electrons. The angular distributions at different incident energies in the range 21.0–25.0 eV are indistinguishable.

guishable as to shape, and thus we plot only a single curve, representative of this range of energies. The monotonic behavior should be noted.

The shape of the angular dependence for the first vibrational state, shown in Fig. 9 also shows, over-all, a monotonic behavior with angle. Figure 10 shows the angular dependence for electrons

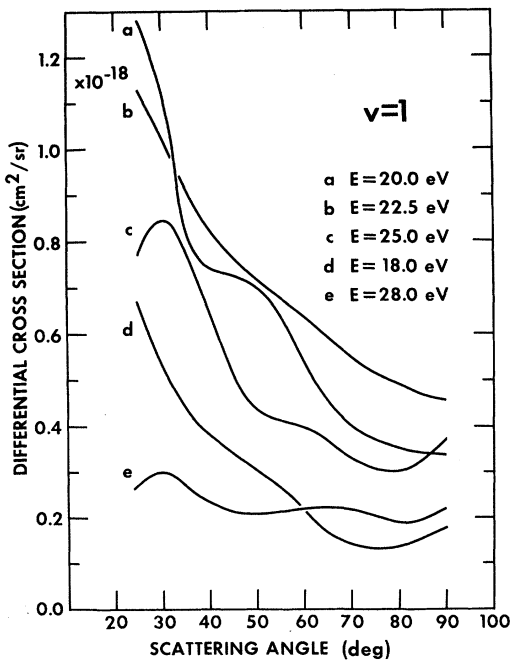

FIG. 9. Angular distribution for electrons having excited the $v=1$ state in N_2.

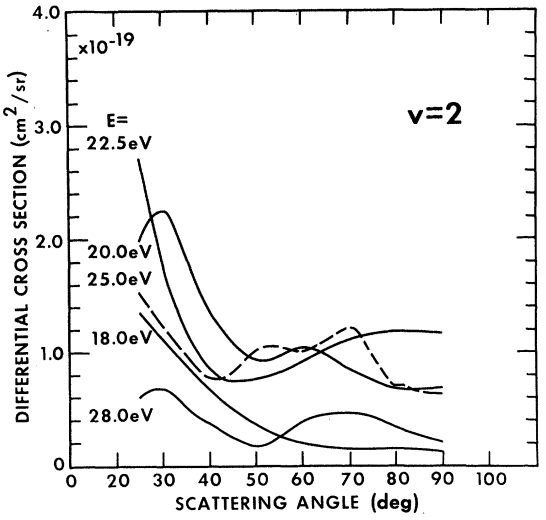

FIG. 10. Angular distribution for electrons having excited the $v=2$ state in N_2.

having excited the $v=2$ state of nitrogen. At an incident energy of 18.0 eV, a monotonically decreasing function is evident. At higher energies, i.e., for 20.0, 22.5, and 25.0 eV, the angular dependence shows an extremely complex structure, indicating the possibility that many overlapping compound states are present. A similar interpretation can be associated with the angular distribution for electrons having excited the $v=3$ state of nitrogen, as shown in Fig. 11.

IV. DISCUSSION

Two features of the results presented in Sec. III are noteworthy: (i) The vibrational cross

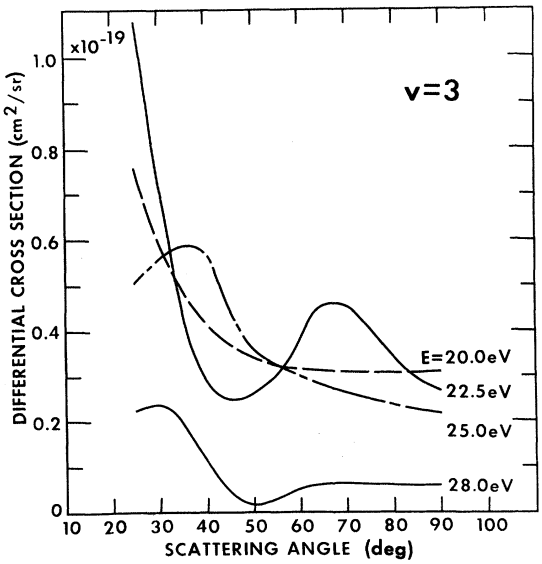

FIG. 11. Angular distribution for electrons having excited the $v=3$ state in N_2.

section for $v=1-3$ in the neighborhood of 22.5 eV is very large; (ii) the angular distribution for electrons having excited the $v=2$ and $v=3$ state of N_2 varies considerably as the electron energy is varied. In Fig. 12 we combine the energy dependence and the angular dependence for $v=2$ into a single plot so as to present pictorially the complexity of the process being studied. As has already been shown in Figs. 6 and 10, the energy dependence of the cross section for $v=2$ (and also for $v=3$) depends on the angle of observation and the angular distribution depends on the electron energy. Possibly the most prominent feature of Fig. 12 is the occurrence of a "hump" in the energy dependence at intermediate angles of observation. It thus appears that the angular distribution in the energy range 20–25 eV is not characteristic of a single partial wave, but it appears to be a superposition of many resonant partial waves.

On the low-energy and the high-energy sides of Fig. 12, the cross section is very much reduced in magnitude, and the angular dependences show a smooth monotonic behavior with a peak in the forward direction. Since N_2 does not possess a permanent dipole moment these contributions to the cross section probably arise from higher-multipole interactions.

The experimental results described above lead us to the possibility that many compound states exist in the neighborhood of 22 eV and that their spacing is so close that it is difficult to resolve them.

These compound states are unlikely to bear much relation to the ionization potentials (at 15.6, 16.7, 18.8, and 23.6 eV), because the cross sections in Figs. 5–7 show no pronounced structure there. *Rydberg* excited states are known to form compound states lying below their parents[21] and shorter-lived compound states lying above their parents. In addition, there is also the possibility that *valence* excited states form compound states.[22] To estimate their density, consider the valence states of N_2 and N_2^-. There are eight valence orbitals available in N_2 and N_2^-, which can be constructured from atomic $2s$ and $2p$ states; they are, in order of ascending energy, $(\sigma_g 2s)$, $(\sigma_u 2s)$, $(\pi_u 2_p)$ (doubly degenerate), $(\sigma_g 2p)$, $(\pi_g 2p)$ (doubly degenerate), and $(\sigma_u 2p)$. The lowest five of these orbitals are filled in the N_2 ground state, which has a configuration $KK(\sigma_g 2s)^2(\sigma_u 2s)^2(\sigma_g 2p)^2(\pi_u 2p)^4$; the uppermost three are empty. Following the nomenclature customary in solid-state and nuclear physics, we shall use the term "hole state" for

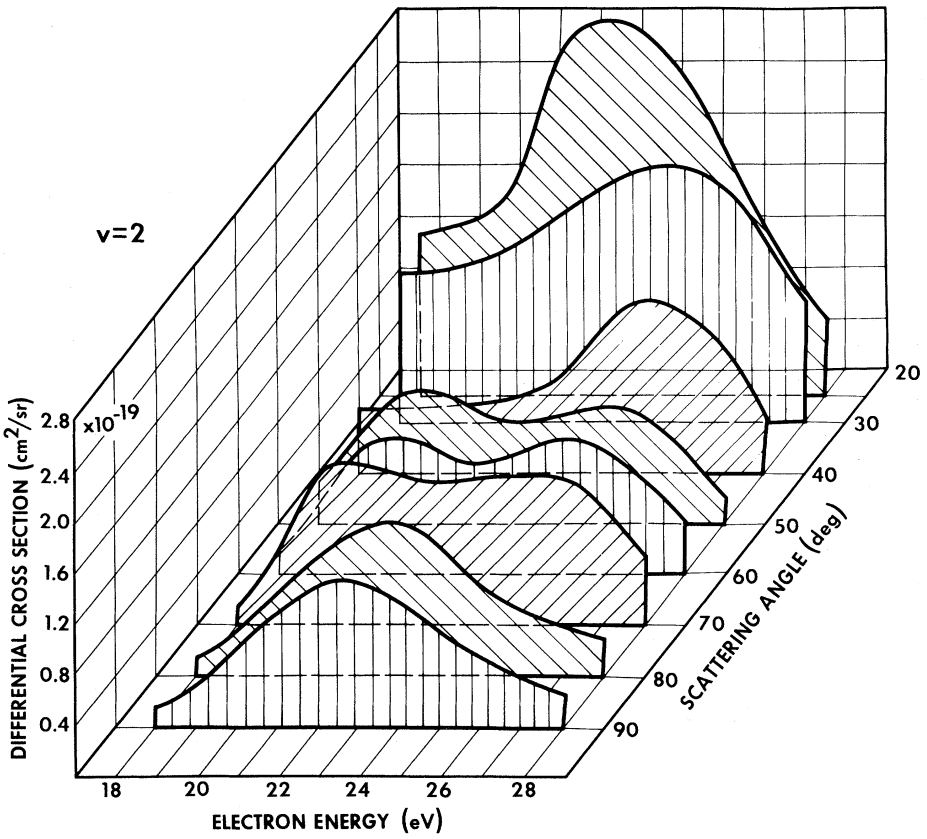

FIG. 12. Combined energy and angular dependence of the differential cross section for vibrational excitation to $v=2$ in N_2.

the occupied orbitals $(\sigma_g 2s)$, $(\sigma_u 2s)$, $(\pi_u 2p)$, and $(\sigma_g 2p)$; and we shall use the term "particle state" for the valence orbitals which are empty in N_2, i.e., $(\pi_g 2p)$ and $(\sigma_u 2p)$. The valence *excited* states of N_2 have n electrons in particle states, where $1 \leq n \leq 6$, and correspondingly n vacancies in hole states; as in solid-state and nuclear physics, we shall say that such an excited state has n "particles" and n "holes", or n "particle-hole pairs".

The *ground* state of the negative ion N_2^- has one particle and no holes. It is an autoionizing compound state (near 1.8 eV) which can decay to various vibrational levels of N_2 by emitting an electron; in the nomenclature customary in electron scattering, it is called a "single-particle resonance" or "shape resonance". There is another such "shape resonance" consisting of a filled N_2 core and a single $(\sigma_u 2p)$ particle, which has not been identified to date. It is probably very broad. N_2 must have also excited valence states which possess n particles, where $6 > n > 1$, and $(n-1)$ holes; if $n = 2$, one has a single extra electron attached to an N_2 valence state with a single particle-hole pair. Conventionally, this would be a "core-excited resonance"; having in mind the single particle-hole pair, we shall call this state a *"singly core-excited resonance"*. Other valence excited states of N_2^- can have from 2 to 5 particle-hole pairs; following the usual nomenclature of electron scattering, one might call the state with two particle-hole pairs a *"doubly core-excited resonance,"* and so on with $n > 2$.

All these states have autoionization widths which arise in part from the ability of the electrons in the higher orbitals, $(\pi_g 2p)$ and $(\sigma_u 2p)$, to tunnel through the centrifugal barriers ($l = 2$ and $l = 1$), and in part from an Auger process in which one electron is emitted while one or more others drop into lower orbitals. In the N_2^- ground state, the tunneling width of the $(\pi_g 2p)$ orbital is 0.6 eV at the equilibrium separation of N_2, and falls rapidly as the separation increases.[10] This tunneling width is extremely sensitive to the energy of the emerging electron, and therefore to correlation effects because they determine the energies of the states; for example, in the ground state of O_2^- in which the extra electron occupies a similar $(\pi_g 2p)$ orbital, the tunneling width is $\ll 0.1$ eV, since O_2^- has good vibrational levels. Therefore, one would expect the tunneling contribution of the (up to four) electrons in the $(\pi_g 2p)$ orbital to the width to vary from about $(0.6 \text{ eV}) \times 4 = 2.4$ eV (for four electrons) downwards. The tunneling width of the $(\sigma_u 2p)$ should be larger than for the $(\pi_g 2p)$, because the energy is higher and the lowest angular momentum component smaller [$l = 1$ instead of $l = 2$ for $(\pi_g 2p)$]. Therefore, states with $(\sigma_u 2p)$ particles should generally be very broad with tunneling widths of several electron volts. The Auger widths are almost unknown; as a guide to their magnitude one has only the existence of many Feshbach resonances in different systems, while lie below their parents in energy; they decay by the Auger process and generally have widths appreciably below 1 eV. We conclude that the widths of valence states should vary from several electron volts for states with $(\sigma_u 2p)$ particles, down to a fraction of an electron volt for some states containing only $(\pi_g 2p)$ particles. Values of a volt or so for the autoionization width are consistent with the observed ratios $\sigma_{v=1}:\sigma_{v=2}:\sigma_{v=3} \simeq 12:3:1$ at 90°, according to Figs. 5–7; this rapid falloff of σ_v, as v rises, suggests that the change of the nuclear separation during the lifetime of the compound states is not large compared with the zero-point amplitude; in fact, the excitation cross sections fall off with the vibrational quantum number a little less rapidly than for the $^2\Sigma_u^+$ resonance in $e + H_2$ at about 3 eV, which has a width of order 3 eV.

The many compound states, which we suggest as being responsible for the observed peak in the vibrational excitation cross sections, could arise in the following way. A straightforward count of states with spin $\frac{1}{2}$ (which are the only ones to be found in e-N_2 scattering) gives 3, 45, 210, 390, 285, and 75 levels with n particles and $n-1$ holes in valence orbitals, where[23] $n = 1, 2, 3, 4, 5$, and 6. An examination of the low-lying spectrum of N_2 and N_2^+ suggests 11 eV as an average excitation energy for the creation of a single particle-hole apir. The excitation energies for states with a given number of particle-hole pairs will spread over a few electron volts because of the fluctuations in the creation energies for the different particle-hole pairs, and the different ways they can be coupled. But, very roughly, one might expect about three N_2^- shape resonances with $n = 1$ in the interval of 11 eV centered at the ground state, about 45 singly core-excited N_2^- states in the next interval from $(2.3 + \frac{11}{2}) = 7.8$ eV to $(2.3 + \frac{3}{2} \times 11) = 18.8$ eV, about 210 doubly core-excited states in the next interval from 18.8 to 29.8 eV, and so on. Clearly, the expected average spacing of valence states around 22 eV should be of the order of $(11 \text{ eV})/210 \approx 0.05$ eV. This level density comes from *all* compound valence states, and includes the broad ones arising from the $(\sigma_u 2p)$ particles. Any direct measurement of the level density with an energy resolution of less than 1 eV, of the kind described in Sec. IV for a 1-eV interval at 21 eV, would observe only a fraction of the level density coming predominantly from the $(\pi_g 2p)$ particles. In addition, there is a contribution from the occupation of higher (i.e., Rydberg) orbitals. (The relative importance of these compound states is discussed in the Appendix.) At present, we can

conclude only that the suggestion of an experimental structure near 21 eV with a spacing of order 0.2 eV is not inconsistent with the theoretical guesses about the level density.

A possible reason why the levels contributing to Figs. 5–7 should be bunched in an interval as narrow as 7 eV (from 18 to 25 eV) follows from considering the compound levels as a thermal equilibrium, as is done in the statistical model of the nucleus.[24] The cross section for scattering to a final state f through such compound states should then have the approximate form $\sigma = \sigma_c P_f$, where σ_c is the cross section for the formation of the complex, and P_f the probability for decay into the final electronic state f, which would be akin to evaporation. The peak in the cross-section curves in Figs. 5–7 could arise in the following way: The level count quoted above (i.e., 3, 45, 210, ... levels for $n = 1, 2, 3, \ldots$) suggests a rapid rise of the level density of N_2^- at a bombarding energy around 15 eV; therefore σ_c should start to rise there, probably saturating at a value of the order of 10^{-16} cm^2, due to the finite size of the molecule. At low incident energies, the value of P_f starts at unity because only the electronic ground state is accessible for decay of the complex, and P_f falls rapidly around 20 eV as more N_2 states become accessible, since the level density of N_2 must also rise rapidly in that region. The product $\sigma_c P_f$ would then show a peak.

It is implicit in this model that the compound states should be able to decay also to excited N_2 states, and that the part of the corresponding cross section arising from compound-state formation should have a peak for each such state, although possibly of a different width from the electronic ground state.

The idea of compound states involving the excitation of several electrons is not new. Several triply excited states are known[25] in He^- at a bombarding energy of about 57 eV for electrons on He. The number of levels and of electrons is much smaller in He^- than in N_2^-.

Vibrational excitation of N_2 at higher energies has been previously observed: Skerbele, Dillon, and Lassettre[26] have studied vibrational excitation at a single electron energy, namely 45 eV by observing forward-scattered electrons between 3° and 14°. They observe a relatively large vibrational cross section, and they find that the intensity of the vibrational peak is a constant fraction of the elastic peak, independent of the scattering angle between 3° and 14°. Our own experiment confirms these findings. We also agree with the interpretation of Skerbele *et al.*, namely, that this process does not involve a compound state and that direct processes such as quadrupole transitions should be invoked.

It is possible that the large vibrational cross section in O_2, observed by Trajmar, Cartwright, and Williams[12] at energies of 10 and 15 eV could also be caused by the contribution of high-lying resonances, but their final data are not yet available.

ACKNOWLEDGMENT

The authors are indebted to L. Sanche for fruitful comments.

APPENDIX: RELATIVE IMPORTANCE OF RESONANCES ASSOCIATED WITH RYDBERG AND VALENCE STATES

In comparing the relative importance of different compound states (Rydberg and valence states for example), it is worth noting that the contribution of any compound state to the total cross section is determined essentially by the entry width. To see this, consider a compound state at energy E_0, with total width Γ_0 and entry width $\Gamma_{0\,\mathrm{in}}$; let σ_T be the total cross section. The contribution of the compound state at E_0 to σ_T contains the energy E in a Breit-Wigner factor,

$$\lambda\!\!\!^{-2}\,\Gamma_{0\,\mathrm{in}}\,\Gamma_0/[(E-E_0)^2+\tfrac{1}{4}\Gamma_0^2],$$

where $\lambda\!\!\!^{-}$ is the incident de Broglie wavelength. If, as in the present experiments, the compound states cannot be observed individually, it is appropriate to consider the average $\bar{\sigma}_T$ of σ_T over an energy interval containing many resonances, i.e.,

$$\bar{\sigma}_T = (1/\Delta)\int_{E-\Delta/2}^{E+\Delta/2} \sigma_T(E')\,dE' .$$

If $\Delta \gg \Gamma_0$, the contribution of the resonance at E_0 to $\bar{\sigma}_T(E)$ is $2\pi\lambda\!\!\!^{-2}\,\Gamma_{0\,\mathrm{in}}/\Delta$. (This argument ignores interference terms between different resonances, which is permissible if the compound states differ sufficiently for the relative phases to be random.)

In general, a negative-ion compound state in which some of the electrons occupy Rydberg orbitals has a smaller $\Gamma_{0\,\mathrm{in}}$ than a compound state with the same number of excited electrons, but all in valence states. In making such comparisons, we consider the *sum over all the vibrational states associated with each electronic state*; then all influence of the vibrational states disappears because the sum of the Franck-Condon factors is unity.[27] All that is important is the overlap of the electronic wave functions. The larger spatial extent of the Rydberg orbitals makes their electronic overlap integrals with the target wave function and the incident wave (which enters into $\Gamma_{0\,\mathrm{in}}$) smaller than the corresponding overlap integrals with the more localized valence orbitals.

We stress that these considerations apply to the *sum* over all vibrational states, and not to the detection of individual vibrational states.

*Work supported by the U. S. National Science Foundation.

†Permanent address: Institute "Ruder Boskovic," Zagreb 41001, Croatia, Yugoslavia.

[1]J. N. Bardsley and F. Mandl, Rept. Progr. Phys. (Kyoto) 31, 471 (1968).

[2]J. C. Y. Chen, *Advances in Radiation Chemistry*, Vol. 1, edited by M. Burton and J. L. Magee (Wiley, New York, 1969), p. 245.

[3]A. Herzenberg, *Methods and Problems of Theoretical Physics*, edited by J. E. Bowcock (North-Holland, Amsterdam, 1967) (in honor of R. E. Peierls).

[4]H. S. W. Massey and E. H. S. Burhop, *Electronic and Ionic Impact Phenomena*, 2nd ed. (Clarendon, Oxford, England, 1969).

[5]A. V. Phelps, Rev. Mod. Phys. 40, 399 (1968).

[6]H. S. Taylor, Advan. Chem. Phys. 18, 91 (1970).

[7]J. Comer and F. H. Read, J. Phys. B 4, 368 (1971).

[8]H. Ehrhardt, L. Langhans, F. Linder, and H. S. Taylor, Phys. Rev. 173, 223 (1968).

[9]For experimental data, see G. J. Schulz, Phys. Rev. 135, A988 (1964); H. Ehrhardt and K. Willmann, Z. Physik 204, 462 (1967).

[10]For a discussion of the theory, see J. C. Y. Chen, in *Advances in Radiation Chemistry*, edited by M. Burton and J. L. Magee (Wiley, New York, 1969), Vol. 1, p. 245; also J. B. Hasted and A. M. Awan, J. Phys. B 2, 367 (1969); D. T. Birtwistle and A. Herzenberg, J. Phys. B 4, 53 (1971).

[11]J. Comer and F. H. Read, J. Phys. B 4, 1055 (1971).

[12]S. Trajmar, D. C. Cartwright, and W. Williams, Phys. Rev. A 4, 1482 (1971).

[13]F. H. Read, J. Phys. E 3, 127 (1970).

[14]P. Marmet and L. Kerwin, Can. J. Phys. 38, 787 (1960).

[15]L. Sanche and G. J. Schulz, Phys. Rev. A 5, 1672 (1972).

[16]R. Herzog, Z. Physik 47, 596 (1935).

[17]F. Rosebury, *Handbook of Electron Tube and Vacuum Techniques* (Addison-Wesley, Reading, Mass., 1965), p. 10.

[18]H. G. M. Heideman, C. E. Kuyatt, G. E. Chamberlain, J. Chem. Phys. 44, 355 (1966).

[19]R. W. LaBahn and J. Callaway, Phys. Rev. A 2, 366 (1970).

[20]A Bayard-Alpert ionization gauge was used on the low-pressure side of the system. It had been calibrated against a Baratron gauge for the ratio of sensitivity between nitrogen and helium. This ratio, $S(N_2)/S(\mathrm{He})$ is found to be 5.67, in excellent agreement with the ratio of 5.55 found by Utterback and Griffith [N. G. Utterback and T. Griffith, Jr., Rev. Sci. Instr. 37, 866 (1966)].

[21]A. W. Weiss and M. Krauss, J. Chem. Phys. 52, 4363 (1970) point out that preferentially Rydberg states lead to sharp (i.e., long-lived) compound states. For an experimental verification, see, e.g., L. Sanche and G. J. Schulz, Phys. Rev. Letters 27, 1333 (1971). However, when Rydberg states are predissociated, they could be broadened.

[22]There is a simple example of a molecular-negative-ion compound state which involves target excitation and which has all the electrons in valence orbitals (as distinct from Rydberg orbitals). This is the $^2\Sigma_g^+$ state of H_2^- observed in the reaction $H_2 + e \rightarrow H_2^- \rightarrow H + H^-$ at about 10 eV (see Refs. 1–4). There are only two valence orbitals: the bonding orbital $(1s+1s)$ and the antibonding orbital $(1s-1s)$; the structure of the H_2^- state is $(1s-1s)^2(1s+1s)$. In the nomenclature of particles and holes used below, it has $n=2$, that is two particles and one hole. As the separation of the nuclei varies, the state moves in energy from above to below its H_2 parent state, $^3\Sigma_u^+(1s+1s)(1s-1s)$.

[23]All the levels considered have spin $\frac{1}{2}$. States which differ in the sign of the angular momentum about the symmetry axis have been counted separately. The two spin projections for each state have been counted as a single state. Our procedure is consistent with that given by R. S. Mulliken, *The Threshold of Space* (Pergamon, New York, 1957), p. 169. However, Mulliken points out that he lists completely only states with holes in the outer two orbitals. Our considerations involve excitation of all valence electrons.

[24]K. J. LeCouteur, in *Nuclear Reactions*, edited by P. M. Endt and M. Demeur (North-Holland, Amsterdam, 1959).

[25]C. E. Kuyatt, J. A. Simpson, and S. R. Mielczarek, Phys. Rev. 138, A385 (1965). See also P. D. Burrow and G. J. Schulz, Phys. Rev. Letters 22, 1271 (1969). Resonances around 57 eV in helium involve three "particles" and two "holes," and the corresponding states in N_2 have $n=3$ and there are 210 of such states.

[26]A. Skerbele, M. A. Dillon, and E. N. Lassettre, J. Chem. Phys. 49 3543 (1968).

[27]G. Herzberg, *Spectra of Diatomic Molecules* (Van Nostrand, Princeton, N. J., 1967), p. 203.